

## Original Research

# Spontaneous Cardiac Calcinosis in BALB/cByJ Mice

Aaron M Glass, Wanda Coombs, and Steven M Taffet\*

BALB/c mice are predisposed to dystrophic cardiac calcinosis—the mineralization of cardiac tissues, especially the right ventricular epicardium. In previous reports, the disease appeared in aged animals and had an unknown etiology. In the current study, we report a substrain of BALB/c mice (BALB/cByJ) that develops disease early and with high frequency. Here we analyzed hearts grossly to identify the presence and measure the severity of disease and to compare BALB/c substrains. Histologic analysis and fluorescent and immunofluorescent microscopy were used to characterize the calcinotic lesions. BALB/cByJ mice exhibited more frequent and severe calcium deposition than did BALB/c mice of other substrains (90% compared with 3% at 5 wk). At this age, lesions covered an average of 30% of the total ventricular surface area in BALB/cByJ mice, compared with less than 1% in other strains. In bone-marrow–chimeric mice, green fluorescent protein was used as a marker to show that the lesions contain an infiltration of cells of bone marrow origin. Lesion histology showed that calcium deposits were surrounded by fibrosis with interspersed immune cells. Lymphocytes, macrophages, and granulocytes were all present. Internalization of the gap-junction protein connexin 43 was observed in myocytes adjacent to lesions. In conclusion, BALB/cByJ mice exhibit more frequent and severe dystrophic cardiac calcinosis than do other BALB/c substrains. Our findings suggest that immune cells are actively recruited to lesions and that myocyte gap junctions are altered near lesions.

**Abbreviations:** Cx43, connexin 43; DCC, dystrophic cardiac calcinosis; GFP, green fluorescent protein.

Calcification of soft tissues can be broadly divided into 2 categories: dystrophic mineralization, which is associated with degenerative conditions including chronic inflammation, and metastatic mineralization, which occurs in response to disrupted calcium or phosphate metabolism. Ectopic mineralization accompanies many cardiovascular disease processes, including atherosclerosis. Dystrophic calcification of heart tissues has been observed in several species, including humans<sup>10</sup> and mice.<sup>8</sup> Several inbred mouse strains, including BALB/c, DBA, and C3H, are reportedly susceptible to spontaneous cardiac calcification.<sup>24</sup> This disorder manifests as focal, calcium-laden lesions, which are often so prominent that they can be observed without visual aid.<sup>9,18</sup> Here we describe the appearance of spontaneous dystrophic mineralization in the BALB/cByJ mouse strain.

BALB/c mice are particularly susceptible to cardiac calcinosis. A study in 1975 included 3360 BALB/cStCrL mice and reported that 10.5% of male mice and 3.6% of female mice had histologic evidence of calcinosis.<sup>11</sup> Similarly, in 1976, a manuscript described spontaneous lesions in 60% of female and 30% of male BALB/cCr mice assessed at 2 mo of age.<sup>4</sup> Other authors noted that calcinosis in BALB/c mice developed later in life, with a mean age of onset of 110 to 150 d in male mice.<sup>9</sup> They noted that among the strains of mice included in their study, BALB/c mice were unique in that they developed calcinosis of the right ventricular epicardium.<sup>9</sup> These studies evaluated disease in specific substrains of BALB/c but did not examine differences among various substrains.

In the current study, we have identified a substrain of BALB/c mice, BALB/cByJ, that uniquely develops a severe epicardial calcinosis, when compared with BALB/c mice from other sources or with other substrains. Mineralized lesions in BALB/cByJ mice contained numerous immune cells, including lymphocytes and macrophages. Analysis of myocytes adjacent to the lesions by immunofluorescence microscopy revealed alterations to the cardiac gap junction protein connexin 43 (Cx43), which forms intercellular channels responsible for allowing the propagation of action potentials and passage of metabolic secondary messengers between cardiac myocytes.<sup>23</sup> These changes may be indicative of an ongoing cycle of tissue destruction.

## Materials and Methods

**Animals.** BALB/cByJ, BALB/cJ, C3H/HeJ, and DBA/2J mice were purchased from The Jackson Laboratory (Bar Harbor, ME); BALB/cAnTac mice were from Taconic (Hudson, NY); and BALB/cAnNCR mice were obtained from NIH (Bethesda, MD). Mice expressing green fluorescent protein (GFP) under the human ubiquitin C promoter of the strain CByJ.B6-Tg(UBC-GFP)30Scha/J were purchased from The Jackson Laboratory. All animals used in this study were male. Most animals that were examined for the presence of lesions were euthanized on or near (within 2 d) the day of their arrival at our facility; mice appeared healthy and did not exhibit any outward signs suggestive of disease. Animals were housed under SPF conditions at the Department of Laboratory Animal Resources of Upstate Medical University. All procedures were IACUC-approved. Husbandry at our facility was identical in regard to water, food, bedding, and stocking density for all mice in our study. Based on information from the suppliers

Received: 21 May 2012. Revision requested: 19 Jun 2012. Accepted: 16 Jul 2012.  
Department of Microbiology and Immunology, SUNY Upstate Medical University,  
Syracuse, New York.

\*Corresponding author. Email: taffets@upstate.edu

of the mice, they received rodent chow ad libitum, which contained similar levels of vitamin D, calcium, and phosphorus, both at the source and once housed at our facility.

**Evaluation of lesion severity.** Immediately after euthanasia, hearts were removed by dissection, flushed with ice-cold PBS, and immediately placed in fresh 1% formaldehyde in PBS. Hearts were examined at a magnification of 2× under a dissecting microscope fitted with a digital camera. Each specimen was photographed at least 4 times, to produce a montage of images covering the entire surface area of the heart. Total ventricular area and lesional area were measured by using ImageJ software (rsbweb.nih.gov/ij/). Statistical analysis was performed by using one-way ANOVA followed by a Bonferroni posttest (Prism, GraphPad Software, La Jolla, CA).

**Paraffin sections.** Hearts were fixed in formalin solution overnight at 4 °C, followed by processing for paraffin embedding by standard procedures and staining with hematoxylin and eosin, Alizarin red S, and Masson trichrome. Bright-field microscopy was performed on an Eclipse E800 microscope (Nikon, Tokyo, Japan) equipped with a SPOT RT Slider (SPOT Imaging Solutions, Sterling Heights, MI) digital camera.

**Immunofluorescence on paraffin sections.** Rehydrated sections (15 µm) were subjected to antigen retrieval by using Tris-EDTA solution (pH 9) in a microwave oven. Slides were allowed to cool to room temperature and were washed twice with PBS. Blocking was performed by incubation in normal goat serum in PBS with 0.2% Triton X100 for 1 h at room temperature. Rabbit antiCx43 (dilution, 1:500; catalog no. AB1728, EMD Millipore, Billerica, MA) was diluted in blocking solution and incubated overnight at 4 °C. Sections were incubated with species-specific fluorochrome-conjugated secondary antibodies and cover slips were mounted by using Prolong Gold with DAPI (Invitrogen, Carlsbad, CA). These sections were visualized on a confocal microscope (model LSM510, Zeiss, Oberkochen, Germany). Z-series of myocytes adjacent to and distant from calcinotic lesions were prepared at 0.38 µm for each consecutive z-section.

**Immunofluorescence on cryosections.** Hearts were excised and placed in fresh 1% paraformaldehyde solution, followed by a 2-step series of 15% and 30% sucrose in PBS for cryoprotection. The next day, hearts were frozen in aqueous-based embedding medium (OCT, Tissue-Tek, Sakura Finetek, Torrance, CA) with 2-methyl butane on dry ice and stored at -80 °C until sectioning. Sections (thickness, 7 µm) were prepared and fixed by acetone-methanol treatment for 15 min at -20 °C. Slides were washed in PBS (3 washes for 5 min each) and blocked by using antimouse blocking solution (MOM Solution, Vector Laboratories, Burlingame, CA) with 0.1% Triton X100, according to the manufacturer's instructions. Primary antibodies (rabbit antiCD3, catalog no. ab5690, Abcam, Cambridge, MA; rabbit antimyeloperoxidase, catalog no. RB375A1, Thermo Fisher Scientific, Waltham, MA; rat antiCD4, catalog no. 100402, Biolegend, San Diego, CA; rat antiCD8, catalog no. 100702, Biolegend; rat antiCD11b, catalog no. 64347, Abcam) were diluted 1:50 (MOM Solution, Vector Laboratories) for staining and analysis of paraffin-embedded sections as described earlier; prepared sections were visualized under light microscopy (Eclipse E800, Nikon).

**Sequencing of the *Abcc6* (*Dyscalc1*) gene.** Genomic DNA was extracted from tail biopsies from 2 mice each of the C3H, BALB/c, C57BL/6, DBA (Taconic), and BALB/cByJ (Jackson) mouse strains by using the DNEasy Blood and Tissue kit (Qiagen, Valencia, CA)

according to the manufacturer's protocol. A 156-bp fragment of exon 14 of the *Abcc6* gene was amplified by using Extensor Hi-Fidelity PCR Mastermix (catalog no. Ab0792, Abgene, Thermo Fisher Scientific) and the "del-bp-ex14" primer pair.<sup>1</sup> The products were sequenced in both the forward and reverse directions by the SUNY Upstate DNA Sequencing Core Facility.

**Generation of GFP chimeric mice.** BALB/cByJ mice (age, 3 wk) were irradiated with 2 doses of 450 rads each and then injected retroorbitally with 5 × 10<sup>6</sup> bone marrow cells from GFP-positive donor mice. The mice were maintained on acid water and tetracycline (Terramycin, AgriLabs, St Joseph, MO; 0.5 tablespoon per 250 mL acidified water [pH 3.0, approximately], changed every 2 d) for 1 wk prior to and 1 mo after transplantation. Mice were housed for 8 wk to allow for hematopoietic reconstitution, after which hearts were examined for surface GFP fluorescence (IVIS 50, Caliper-Xenogen, Waltham, MA). After imaging, hearts were cryosectioned and studied for GFP fluorescence by microscopy. To ensure sufficient reconstitution, peripheral blood was examined for GFP fluorescence as described following.

**Flow cytometry.** Peripheral blood was obtained by retroorbital bleed and placed immediately into EDTA anticoagulant tubes (Microvette, Sarstedt, Newton, NC). Erythrocytes were lysed by using ammonium chloride-potassium buffer. Cells were stained with antiCD45 conjugated to phycoerythrin (catalog no. 103105, BioLegend) and examined for GFP fluorescence (to quantify reconstitution of chimeric animals). Alternatively, cells were stained for the minor histocompatibility marker Qa2 by using a FITC-conjugated antibody (catalog no. 11-5996-82, eBioscience, San Diego, CA). Samples were analyzed by flow cytometry, during which at least 1 × 10<sup>4</sup> live cells were collected. Cytometric data were evaluated by using FlowJo software (Tree Star, Ashland, OR).

**CBC analysis.** Peripheral blood was drawn from 10 BALB/cByJ and 4 BALB/cAnTac mice and analyzed in an automated blood analyzer (Hemavet, Drew Scientific, Dallas, TX). The machine was calibrated and a control sample was run and checked prior to each sample batch.

## Results

**Spontaneous epicardial calcinosis appeared at high frequency and severity in BALB/cByJ mice.** After euthanasia, all 12 BALB/cByJ mice and none of the 12 BALB/cAnTac mice analyzed had evidence of calcinosis. In BALB/cByJ mice, mineralization was evident on gross inspection, often manifesting as prominent, white epicardial lesions (Figure 1 A). BALB/c mice and related substrains are known to display similar patterns of calcification.<sup>4,9,11</sup> However, the overall frequency of calcinosis was much higher in BALB/cByJ mice than in other BALB/c substrains. In the present study, 90% of BALB/cByJ mice had disease by 5 wk of age (Table 1). Other BALB/c substrains had much lower frequencies of disease: the BALB/cAnTac strain had a frequency of 3.0%, whereas mice of the BALB/cAnNCR strain were disease-free. The BALB/cByJ line is derived from the progenitors of these 2 strains. The more distant substrain, BALB/cJ, which diverged from the Andervont line in the mid-1930s,<sup>16,25</sup> had much less disease (frequency of 17%) than did BALB/cByJ mice, even though both of these strains were obtained from the same source. We examined kidneys, spleens, and livers from mice of each of these strains but did not note any calcification of these organs. Overall, more than 100 male BALB/cByJ mice at various ages and treatments were examined, and the vast majority had visible signs of disease.

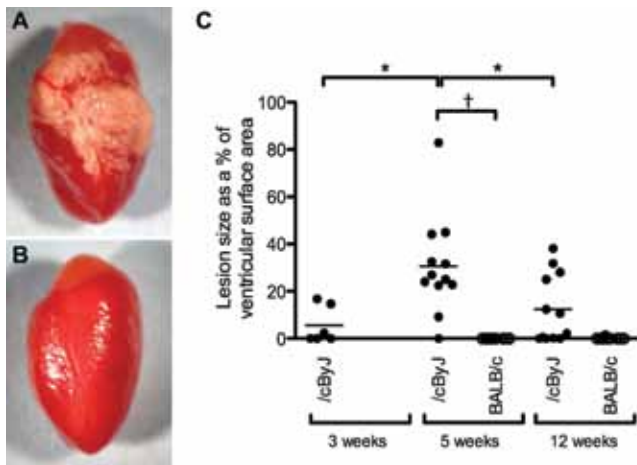


**Figure 1.** BALB/cByJ mice developed severe cardiac calcinosis by 5 wk of age. (A) Gross appearance of a mineralized lesion on the epicardial surface of an affected BALB/cByJ subject. (B) Epicardium of an unaffected BALB/cAnTac mouse. (C) Plot comparing the percentages of the ventricular surface occupied by lesion in BALB/cByJ (/cByJ) mice at 3, 5, and 12 wk and in BALB/c mice at 5 and 12 wk. Each symbol represents a single animal; horizontal lines represent the mean. Statistical significance (\*,  $P < 0.01$ ; †,  $P < 0.001$ ) was determined by using one-way ANOVA followed by the Bonferroni posttest.

**Table 1.** Prevalence of epicardial calcinosis in 5-wk-old mice of BALB/c substrains

	No. of mice with lesions/ total no. of mice	% of hearts with lesions
BALB/NCR	0/7	0.0
BALB/cAnTac	1/33	3.0
BALB/cJ	1/6	16.7
BALB/cByJ	44/49	89.8

In 5-wk-old BALB/cByJ mice, lesions occupied variable percentages of the ventricular surface area (Figure 1 C), ranging from no lesion to 83% of the ventricular surface being affected, with an average of 30% coverage in evaluated animals. In some BALB/cByJ mice, lesions were visible at 3 wk of age, whereas lesions were not present by 12 wk in most of the BALB/c mice examined (Figure 1 C). Because we were unable to study disease progression in individual animals, we could not determine whether this reduction in severity represents resolution of disease in older animals or simply batch-to-batch variation.

**Epicardial lesions contained calcium deposits, collagen fibers, and bone marrow-derived cells.** Histology was performed on hearts from 5-wk-old BALB/cByJ mice. The calcium-specific stain Alizarin red S was used to demonstrate the presence of calcium in the lesions, which occurred mainly on the right ventricular epicardial surface (Figure 2 A). Masson trichrome staining highlighted the presence of abundant collagen fibers surrounding denser-staining mineralized areas (Figure 2 B and C). Staining with hematoxylin and eosin demonstrated degenerating muscle fibers within lesions, many containing cytoplasmic granules that likely represent accumulating calcium. More severe lesions contained compact mineralized foci (Figure 2 D). Much of the lesioned area was highly cellular; both mononuclear cells and eosinophils were observed in many cases (Figure 2 D). Histology of the kidneys of these mice revealed no pathology, and the tissue was negative for calcinosis as assessed by Alizarin red staining (data not shown).

GFP-chimeric mice were generated by transplanting donor GFP-expressing bone marrow cells into BALB/cByJ host mice. In this model system, responding bone marrow cells strongly express the GFP reporter and can easily be differentiated from nonfluorescent host cells and tissues. Peripheral blood from chimeric mice was analyzed by flow cytometry to determine the degree of reconstitution by using GFP fluorescence as a marker for donor-derived cells. On average, donor cells represented 78.4% ± 2.3% of CD45-positive leukocytes (data not shown).

When chimeric hearts were harvested, epicardial lesions exhibited intense GFP fluorescence (Figure 3 B). Subsequently, sections of tissue from chimeric hearts were examined by fluorescence microscopy, and GFP-positive cells were noted prominently within lesions (Figure 3 C and D).

**Cells within lesions expressed myeloperoxidase, CD3, CD4, and CD11b.** Immunofluorescence microscopy was used to further characterize the cells within the calcinotic lesions of BALB/cByJ mice. Cells positive for myeloperoxidase, a marker of myeloid cells (particularly neutrophils), were present (Figure 4 A). In addition, lesions were rich in CD3-positive cells, indicating the presence of T lymphocytes and the possibility of an inflammatory or autoimmune etiology (Figure 4 B through D). Many of these cells were also positive for the  $T_H$  marker, CD4 (Figure 4 B), but CD8-positive cells within lesions were rare (data not shown). Myeloid cells were common, as indicated by lesional areas that contained CD11b-positive cells (Figure 4 D). Despite the inflammation in the heart, we did not note overt leukocytosis in affected BALB/cByJ mice compared with nonaffected BALB/cAnTac mice (data not shown).

**Cardiac myocytes adjacent to calcinotic lesions displayed aberrant subcellular localization of the gap-junction protein Cx43.** The present study was initiated as part of a larger study of the development of arrhythmias during myocarditis. Because calcinotic lesions in BALB/cByJ mice were associated with focal myocarditis, immunofluorescent confocal microscopy was used to localize several proteins involved in cardiac intercalated disks. A consistent finding in BALB/cByJ mice with epicardial lesions was a speckled pattern of Cx43 staining in myocytes adjacent to calcinotic lesions. Cx43 was present at high concentrations at the intercalated disks between myocytes in healthy tissues (Figure 5 A through C). In hearts with lesions, however, Cx43 fluorescence was present in the sarcoplasm of myocytes and in the intercalated disks (Figure 5 D through F). This internalization could represent a failure of Cx43 to localize to the intercalated disk, or the internalized speckles could represent gap junctions undergoing degradation.

**Epicardial calcinosis in BALB/cByJ mice was not due to the *Dyscalc1* gene or Qa2 status.** Cardiac calcinosis occurs in several inbred strains of mice, including BALB/c, C3H, and DBA.<sup>8</sup> Early reports suggested a genetic predisposition for disease development in DBA mice,<sup>5</sup> and several loci were identified by quantitative trait loci analysis in C3H mice, the most important of which is thought to be located on chromosome 7.<sup>17,18</sup> The cause of disease in C3H mice has been reported to be a missense mutation in the *Abcc6* gene.<sup>2</sup> We sequenced several BALB/c substrains, including BALB/cByJ, for this mutation. The previously described mutation was present in DBA and C3H strains but not BALB/c and BALB/cByJ mice (Table 2). In addition, a deletion at the immunoregulatory Qa2 locus has been identified in several BALB/c substrains.<sup>16</sup> Flow cytometry analysis of calcinosis-susceptible BALB/cByJ leukocytes indicated that they did not express Qa2, a phenotype they

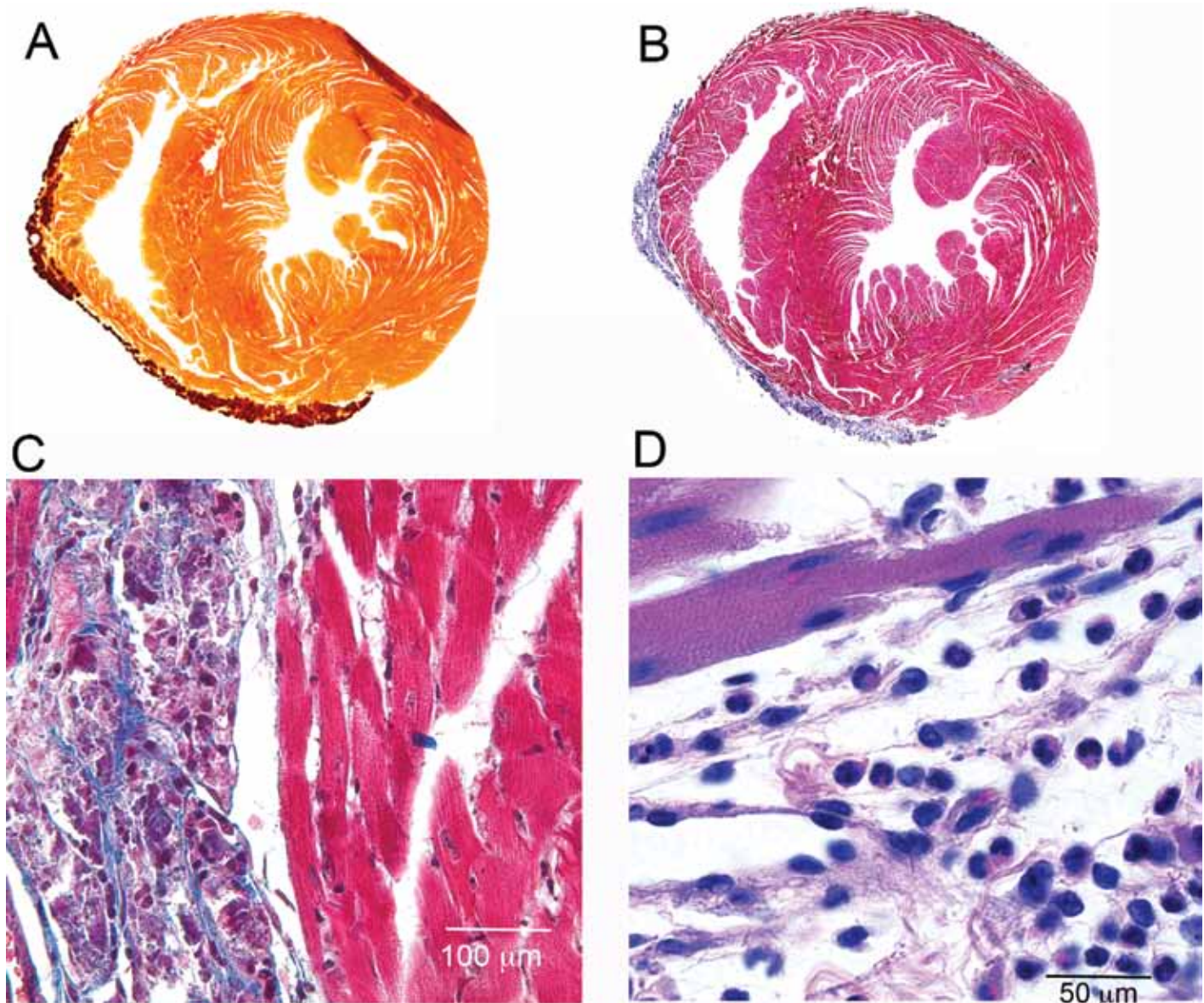


**Figure 2.** BALB/cByJ lesions contained calcium, collagen, and inflammatory cells. (A) BALB/cByJ heart sectioned transversely and stained with Alizarin red S. Orange–brown areas indicate the presence of calcium (darker area at top right is an artifactual fold in the tissue). (B and C) Heart stained with Masson trichrome, showing abundant collagen fibers within lesions. (D) Note the presence of both mononuclear and polymorphonuclear cells; hematoxylin and eosin stain. The images in panels A and B are composites acquired at a magnification of 100 $\times$ .

share with nonsusceptible BALB/cAnTac and BALB/cAnNCR mice (Table 2). We also analyzed serum calcium concentrations in BALB/cByJ mice and compared them with those in BALB/cAnTac mice and found no difference (data not shown). Therefore, the susceptibility of BALB/cByJ mice to calcinosis is not due to a previously described genetic trait.

### Discussion

Although the presence of cardiac calcinosis has been noted among substrains of BALB/c mice, the current study highlights the extremely high frequency of the disease in mice of the BALB/cByJ substrain. Three large studies have focused specifically on BALB/c epicardial mineralization: one found lesions in 10.5% of male BALB/cStCrl mice;<sup>11</sup> another found the frequency to be

7.6% in BALB/cCr mice of both sexes;<sup>20</sup> and the remaining study reported disease in 34% of BALB/c mice. None of these studies compared different substrains from different sources. We compared several related strains of BALB/c mice and found a distinct predisposition for calcinotic lesions among BALB/cByJ mice.

Of the 4 BALB/c substrains we tested, BALB/cByJ mice were most likely to exhibit calcinosis. Another substrain (BALB/cNCR) had no lesions. Disease was much less prevalent in 2 substrains that are closely related to the BALB/cByJ strain, BALB/cAnTac and BALB/cAnNCR, than in their BALB/cByJ counterparts, despite the fact that all 3 substrains are derived from a common line, BALB/cAn. We could not identify a genetic cause for this difference, even though a mutation in *Abcc6* has been identified to correlate with calcinosis in DBA and C3H mice.<sup>1</sup> Despite the

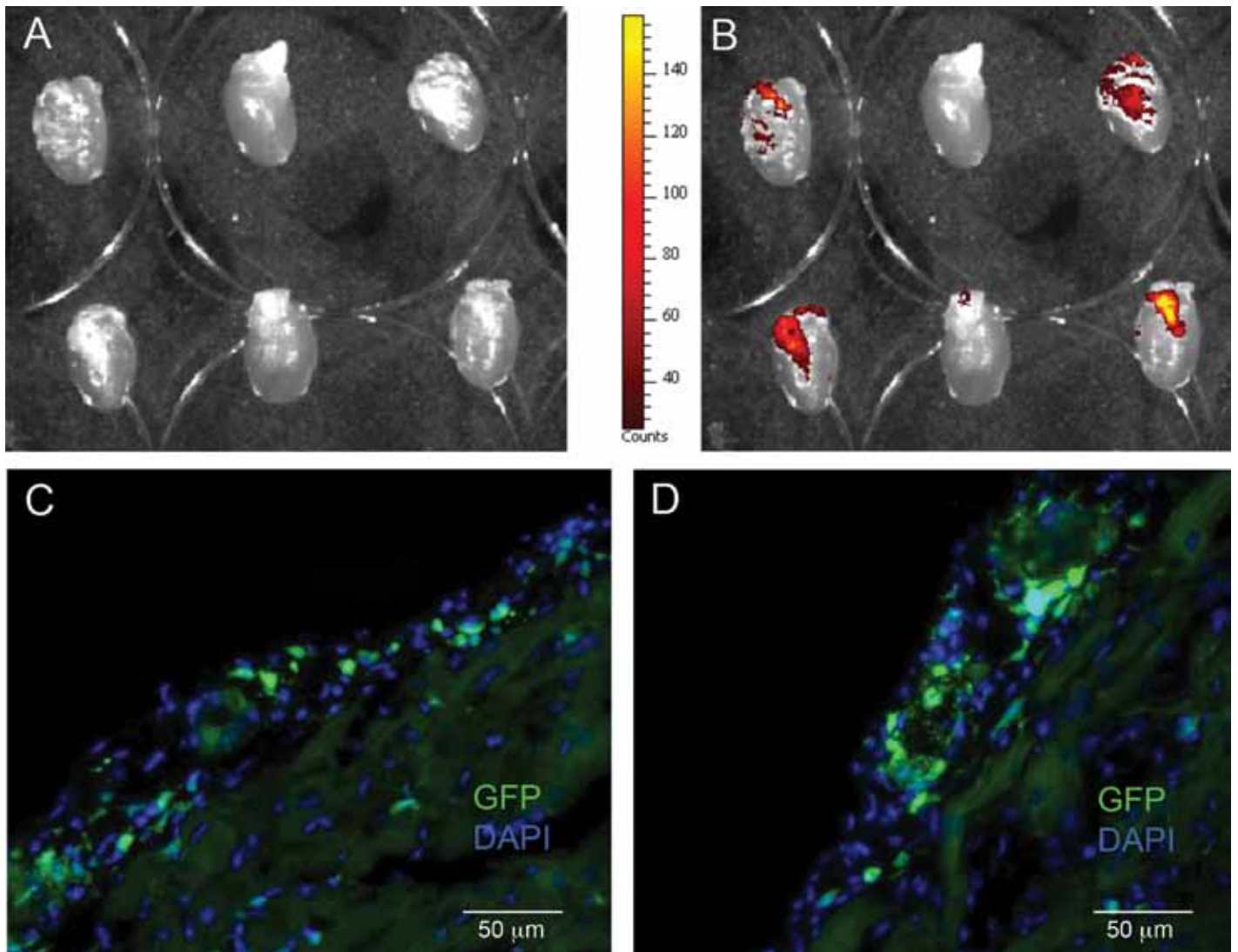


**Figure 3.** Mineralized lesions in BALB/cByJ GFP-chimeric mice were GFP-positive. (A) Exteriors of GFP-chimeric hearts viewed under visible light. (B) Chimeric hearts showing GFP fluorescence pseudocolored in red–yellow, such that red areas fluoresce GFP-positive and yellow areas are strongly GFP-positive. (C and D) Fluorescence microscopy of epicardial lesions showing GFP-positive cells in green and DAPI-stained nuclei in blue. Calibration bars are 50  $\mu\text{m}$ .

relationship between the BALB/c, DBA, and C3H strains (a derivative of the BALB/c line was crossed with a DBA mouse to produce the C3H line),<sup>25</sup> mice of the BALB/c lineages (including BALB/cByJ) do not share this aberrant allele.<sup>25</sup> Similarly, expression levels of the immunoregulatory Qa2 minor histocompatibility molecule did not correlate with development of disease. Therefore, no single gene studied was implicated in the development of calcinosis in BALB/cByJ mice.

The present study focused on young animals (approximate age, 5 wk), resulting in more than 87% of BALB/cByJ mice exhibiting disease. Previous studies have reported that the incidence of mineralized cardiac lesions appears to increase with increasing age.<sup>9,26</sup> The age of onset of disease was calculated in a previous study to be between 16 and 21 wk of age in male BALB/c mice, much older than our BALB/cByJ animals.<sup>9</sup> In the current study, we found that both frequency and severity (in terms of the proportion of ventricular area covered by lesion) significantly increased

from 3 wk to 5 wk but then decreased at 12 wk (Figure 1 C). One explanation for this pattern is the possibility that a subpopulation of the infiltrating immune cells (such as macrophages) acts to resolve the lesions by clearing accumulated mineralization. Macrophages express osteopontin, an inhibitor of calcification, after recruitment to the heart in models of rat and mouse myocardial necrosis initiated by freeze–thaw injury.<sup>1,22</sup> However, a limitation of the current study was that we were unable to track the development (and potential resolution) of disease within a single animal. Therefore, the apparent reductions in incidence and severity, although statistically significant, may simply represent batch-to-batch variation.

Although the exact role of innate immunity in cardiac calcinosis is unclear, the presence of granulocytes (Figure 2 D) and positivity for CD11b and myeloperoxidase (Figure 4) indicate that these cells are commonly found within lesions. Interestingly, most characterizations of dystrophic cardiac calcinosis in mice make no specific

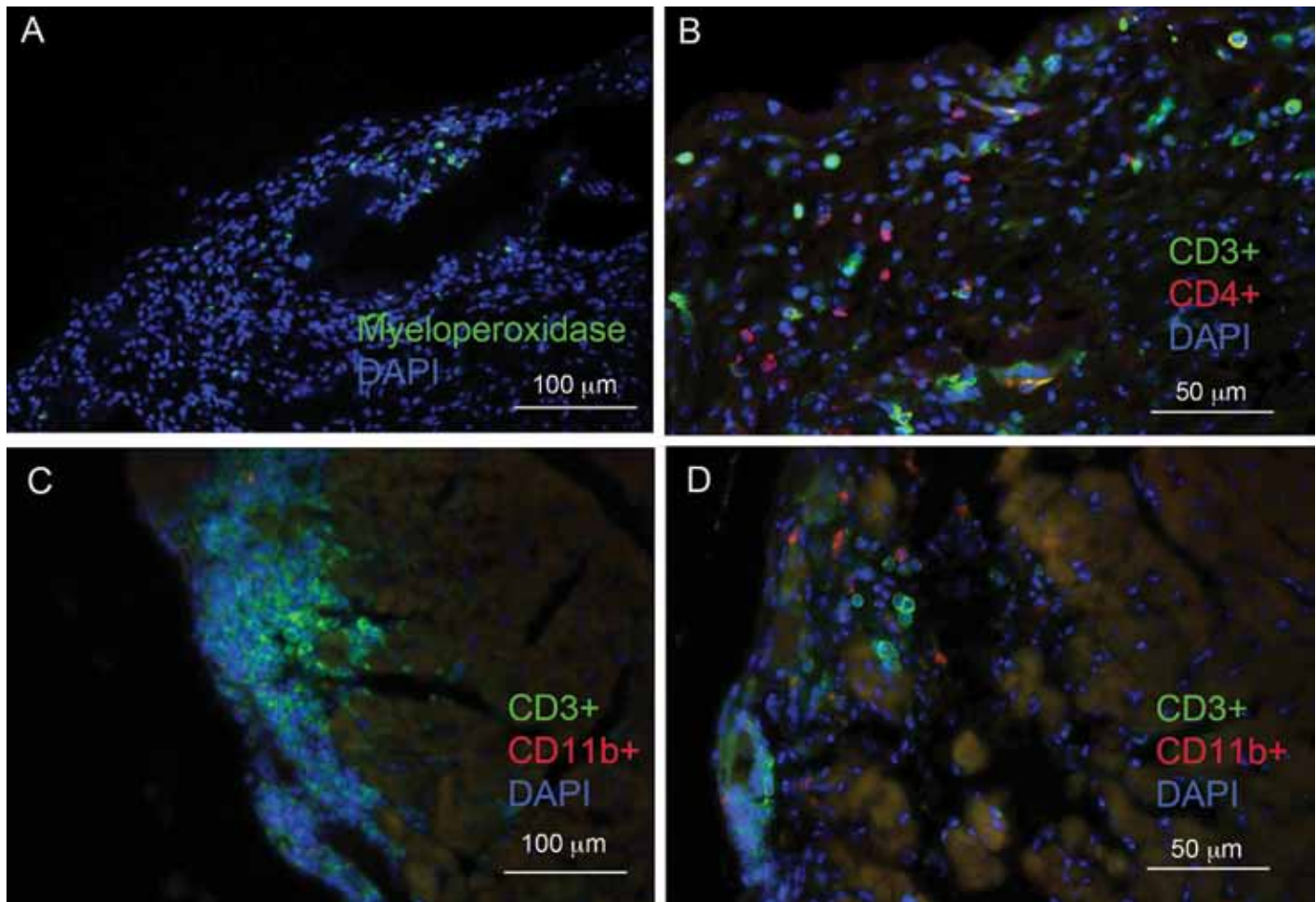


**Figure 4.** Cells within epicardial lesions stained positively for myeloperoxidase, CD3, CD4, and CD11b. (A) Cells shown in green are positive for the neutrophil marker myeloperoxidase. (B) Cells shown in green were positive for the T lymphocyte marker CD3, whereas those in red were positive for CD4. (C and D) Both CD3- and CD11b-staining cells were found within lesions. All sections were counterstained with DAPI (blue)

mention of the accompanying myocarditis that we describe here. This difference may be implicit evidence of phenotypically different types of dystrophic calcinosis in different strains of mice or in different animal models. An earlier study of calcinotic disease in BALB/cCr mice reported the presence of polymorphonuclear and mononuclear cells, even in some cases where identifiable lesions had yet to form.<sup>4</sup> This finding suggests that innate immune cells are present throughout all stages of calcinotic disease, perhaps arriving during the very earliest stages.

The influence of diet on the development of dystrophic calcinosis has been investigated in several studies, and reports have included increasing severity of disease in C3H mice with increasing dietary fat,<sup>9</sup> increased dietary protein levels in DBA mice,<sup>3</sup> and even the administration of tobacco products in feed.<sup>8</sup> In the current study, mice received feed containing essentially the same contents of calcium, phosphorous, and vitamin D when housed at each of the suppliers' facilities and at our own, eliminating the possibility that the differences observed in the development of calcinotic disease arose due to diet. A possibility that our study did not address is the contribution of the intestinal microbial flora to the development of calcinosis. Calcinosis of both cardiac and skeletal muscle can be induced by damage due to physical

trauma<sup>6</sup> or toxins,<sup>32</sup> suggesting that any source of myocyte damage can precipitate calcinosis in predisposed strains. Although a source of damage is not readily apparent in BALB/cByJ mice, an environmental agent could serve as the trigger. Such a situation has been reported in other BALB/c substrains after infection with the murine gammaherpes virus MHV68,<sup>14</sup> encephalomyocarditis virus,<sup>21</sup> murine cytomegalovirus,<sup>12</sup> and *Francisella novicida*.<sup>28</sup> Most of these previous studies were performed in young mice, and the lack of calcium deposits in control animals suggested that either the infectious agent or the associated immune response led to the development of cardiac calcinosis, most likely by causing necrosis of myocytes. In support of an inflammatory hypothesis, we observed marked GFP fluorescence in the calcinotic lesions of BALB/cByJ mice given bone marrow from GFP-expressing donors. One study demonstrated the importance of the spleen as a reservoir of monocytes that could be recruited to sites of myocardial infarction.<sup>31</sup> We found intense GFP fluorescence in the spleens of GFP-chimeric mice (data not shown), perhaps representing monocytes that would eventually have been recruited to developing calcinotic lesions. However, a definitive mechanism for the development of cardiac calcinosis in BALB/cByJ mice has not yet been identified.

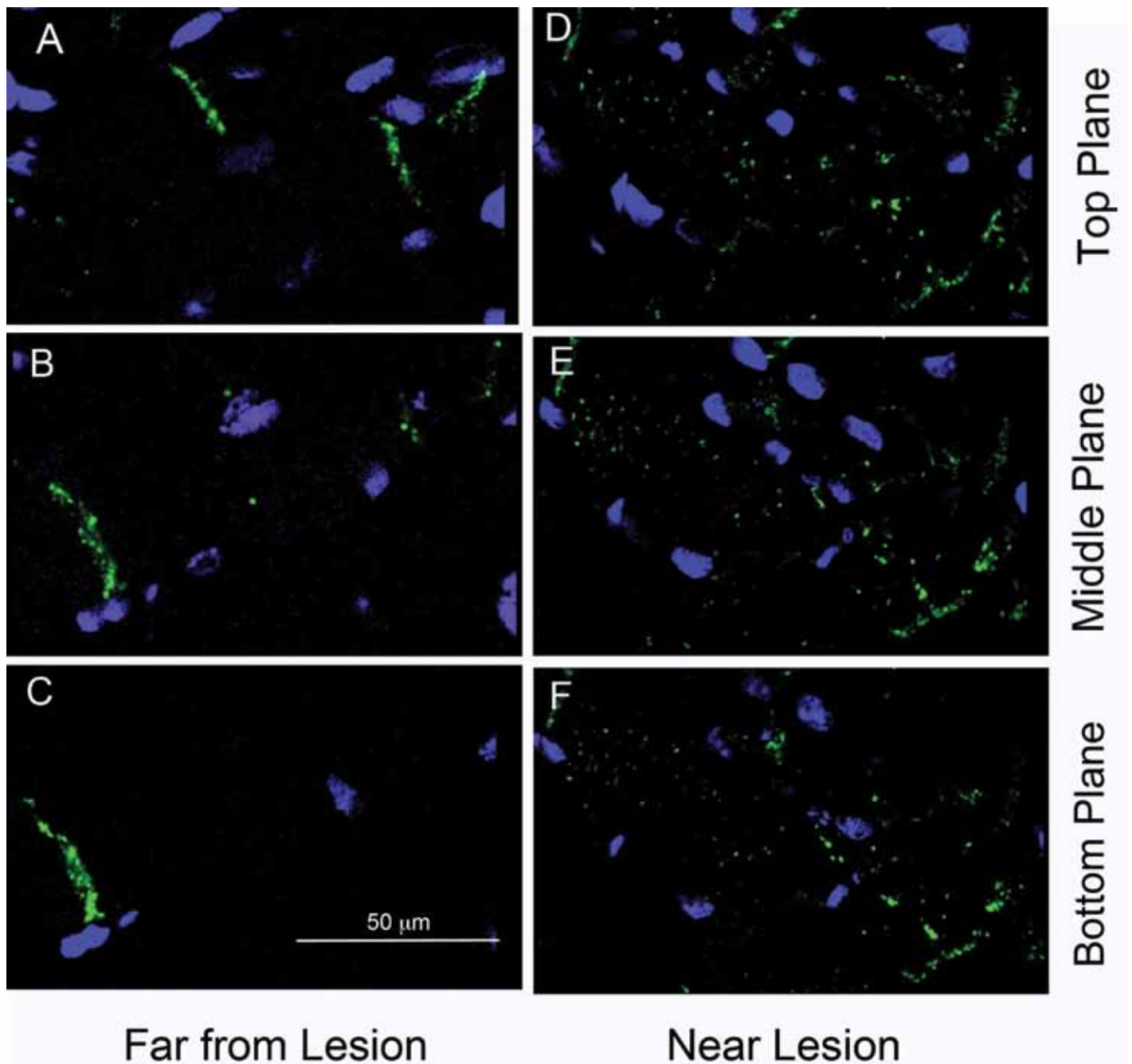


**Figure 5.** Cx43 staining patterns were altered in myocytes adjacent to calcinotic lesions. Z planes are shown in myocytes distant from lesions (A through C) and adjacent to lesions (D through F). Cx43 staining was localized at intercalated disks and within the cytoplasm of myocytes adjacent to lesions.

Humans are susceptible to the development of myocardial calcification, although the condition is rare in humans.<sup>30</sup> In some instances, human calcification is similar to that observed in BALB/c mouse substrains. When visualized by computed tomographic imaging, calcific constrictive pericarditis in humans has a morphology resembling an eggshell and shows similar characteristics to calcinotic disease in mice, including right ventricular predominance.<sup>13,19</sup> Supporting the existence of an infectious or inflammatory etiology, tuberculosis and rheumatoid arthritis are known causes of calcific constrictive pericarditis, although most cases are idiopathic.<sup>27</sup> Therefore,

the spontaneous development of disease in BALB/cByJ mice may serve as a model system in which to study the progression and immune contribution to human calcinotic disease. The possibility that murine cardiac calcinosis arises as part of an inflammatory disease is supported by the large numbers of T lymphocytes in the lesions of BALB/cByJ mice. In addition, we identified numerous macrophages, granulocytes, and CD4+ cells but few CD8+ cells in lesions.

A final interesting aspect of the calcinosis that we identified in the current study was the internalization of the gap-junction protein Cx43 from the intercalated disk to the sarcoplasm of myocytes

**Table 2.** Presence of the dystrophic cardiac calcinosis (DCC) allele and Qa2 expression in several inbred mouse strains

	DCC allele present?	Qa2 expression	Calcinosis present?
C57BL/6	No	High	No
C3H/HeJ	Yes	Not tested	Yes
DBA/2J	Yes	Not tested	Yes
BALB/cAnTac	No	Absent	Low <sup>a</sup>
BALB/cByJ	No	Absent	Yes <sup>a</sup>
BALB/cJ	Not tested	Low	Low <sup>a</sup>

<sup>a</sup>See Table 1.

located near mineralized lesions. Similar Cx43 internalization has been observed in other rodent models of cardiovascular pathology.<sup>15</sup> For example, a model of right ventricular hypertrophy caused by drug-induced pulmonary hypertension demonstrated similar Cx43 internalization and its reduction at the intercalated disk.<sup>29</sup> Similar internalization has been demonstrated in cultured rat myocytes under hypoxia.<sup>7</sup> These studies suggest that Cx43 remodeling by internalization may be a sign of cellular stress. This finding suggests that the myocytes nearest to calcified lesions are undergoing necrosis and eventual calcification. Ultimately, this pattern may represent evidence of a cycle of myocyte death, immune cell recruitment, and calcification.

In conclusion, the broad range of prevalence and severity of spontaneous calcinosis among substrains of BALB/c mice emphasizes their divergence and provides an example of the importance of careful selection of particular substrains and sources of animals for research models. Further studies to investigate the mechanisms behind dystrophic cardiac calcinosis and the associated inflammatory cell infiltration into the myocardium may be warranted.

### Acknowledgments

We thank the following people, without whom this work would not have been possible: Li Gao for her technical skill and expertise; Dr Sandra Hayes for the generous gift of antibodies; Dr Michael Lyon and Linda Steer for their technical expertise and for the use of their cryostat; Dr Mira Krendel for the use of her dissecting microscope; and Josh Satalin and the Department of Surgery at Upstate Medical University for the use of their Roche Cobas blood chemistry analyzer. We also thank Dr Arthur Tatum and Dr Robert Quinn for helpful discussions and suggestions. This work was supported by research grants HL039707 and HL100111 from the NIH.

### References

- Aherrahrou Z, Axtner SB, Kaczmarek PM, Jurat A, Korff S, Doehring LC, Weichenhan D, Katus HA, Ivandic BT. 2004. A locus on chromosome 7 determines dramatic upregulation of osteopontin in dystrophic cardiac calcification in mice. *Am J Pathol* **164**:1379–1387.
- Aherrahrou Z, Doehring LC, Ehlers EM, Liptau H, Depping R, Linsel-Nitschke P, Kaczmarek PM, Erdmann J, Schunkert H. 2008. An alternative splice variant in *Abcc6*, the gene causing dystrophic calcification, leads to protein deficiency in C3H/He mice. *J Biol Chem* **283**:7608–7615.
- Ball CR, Williams WL. 1965. Spontaneous and dietary-induced cardiovascular lesions in DBA mice. *Anat Rec* **152**:199–209.
- Bellini O, Casazza AM, di Marco A. 1976. Histological and histochemical studies of myocardial lesions in BALB/c mice. *Lab Anim Sci* **26**:329–333.
- Brownstein DG. 1983. Genetics of dystrophic epicardial mineralization in DBA/2 mice. *Lab Anim Sci* **33**:247–248.
- Brunnert SR. 1997. Morphologic response of myocardium to freeze-thaw injury in mouse strains with dystrophic cardiac calcification. *Lab Anim Sci* **47**:11–18.
- Danon A, Zeevi-Levin N, Pinkovitch DY, Michaeli T, Berkovich A, Flugelman M, Eldar YC, Rosen MR, Binah O. 2010. Hypoxia causes connexin 43 internalization in neonatal rat ventricular myocytes. *Gen Physiol Biophys* **29**:222–233.
- Dipaolo JA, Strong LC, Moore GE. 1964. Calcareous pericarditis in mice of several genetically related strains. *Proc Soc Exp Biol Med* **115**:496–497.
- Eaton GJ, Custer RP, Johnson FN, Stabenow KT. 1978. Dystrophic cardiac calcinosis in mice: genetic, hormonal, and dietary influences. *Am J Pathol* **90**:173–186.
- Ferguson EC, Berkowitz EA. 2010. Cardiac and pericardial calcifications on chest radiographs. *Clin Radiol* **65**:685–694.
- Frith CH, Haley TJ, Seymore BW. 1975. Spontaneous epicardial mineralization in BALB/cStCrI mice. *Lab Anim Sci* **25**:787.
- Gang DL, Barrett LV, Wilson EJ, Rubin RH, Medearis DN. 1986. Myopericarditis and enhanced dystrophic cardiac calcification in murine cytomegalovirus infection. *Am J Pathol* **124**:207–215.
- Goel PK, Moorthy N. 2011. Tubercular chronic calcific constrictive pericarditis. *Heart Views* **12**:40–41.
- Hausler M, Sellhaus B, Scheithauer S, Gaida B, Kuroepka S, Siepmann K, Panek A, Berg W, Teubner A, Ritter K, Kleines M. 2007. Myocarditis in newborn wildtype BALB/c mice infected with the murine gammaherpesvirus MHV68. *Cardiovasc Res* **76**:323–330.
- Hesketh GG, Shah MH, Halperin VL, Cooke CA, Akar FG, Yen TE, Kass DA, Machamer CE, Van Eyk JE, Tomaselli GF. 2010. Ultrastructure and regulation of lateralized connexin 43 in the failing heart. *Circ Res* **106**:1153–1163.
- Hilgers J, van Nie R, Ivanyi D, Hilkens J, Michalides R, de Moes J, Poort-Keesom R, Kroezen V, von Deimling O, Kominami R, Holmes R. 1985. Genetic differences in BALB/c substrains. *Curr Top Microbiol Immunol* **122**:19–30.
- Ivandic BT, Qiao JH, Machleder D, Liao F, Drake TA, Lusic AJ. 1996. A locus on chromosome 7 determines myocardial cell necrosis and calcification (dystrophic cardiac calcinosis) in mice. *Proc Natl Acad Sci USA* **93**:5483–5488.
- Ivandic BT, Utz HF, Kaczmarek PM, Aherrahrou Z, Axtner SB, Klepsch C, Lusic AJ, Katus HA. 2001. New Dyscalc loci for myocardial cell necrosis and calcification (dystrophic cardiac calcinosis) in mice. *Physiol Genomics* **6**:137–144.
- Ling LH, Oh JK, Breen JF, Schaff HV, Danielson GK, Mahoney DW, Seward JB, Tajik AJ. 2000. Calcific constrictive pericarditis: is it still with us? *Ann Intern Med* **132**:444–450.
- Madison RM, Rabstein LS, Bryan WR. 1968. Mortality rate and spontaneous lesions found in 2928 untreated BALB/cCr mice. *J Natl Cancer Inst* **40**:683–685.
- Matsumori A, Kawai C. 1982. An experimental model for congestive heart failure after encephalomyocarditis virus myocarditis in mice. *Circulation* **65**:1230–1235.
- Murry CE, Giachelli CM, Schwartz SM, Vracko R. 1994. Macrophages express osteopontin during repair of myocardial necrosis. *Am J Pathol* **145**:1450–1462.
- Nguyen TD, Taffet SM. 2009. A model system to study Connexin 43 in the immune system. *Mol Immunol* **46**:2938–2946.
- Percy D, Barthold S. 2001. Pathology of laboratory rodents and rabbits. Ames (IA): Iowa State University Press.
- Potter M. 1985. History of the BALB/c family. *Curr Top Microbiol Immunol* **122**:1–5.
- Rings RW, Wagner JE. 1972. Incidence of cardiac and other soft tissue mineralized lesions in DNA2 mice. *Lab Anim Sci* **22**:344–352.
- Roberts WC. 2005. Pericardial heart disease: its morphologic features and its causes. *Proc (Bayl Univ Med Cent)* **18**:38–55.

28. Roth KM, Oghumu S, Satoskar AA, Gunn JS, van Rooijen N, Satoskar AR. 2008. Respiratory infection with *Francisella novicida* induces rapid dystrophic cardiac calcinosis (DCC). *FEMS Immunol Med Microbiol* **53**:72–78.
29. Sasano C, Honjo H, Takagishi Y, Uzzaman M, Emdad L, Shimizu A, Murata Y, Kamiya K, Kodama I. 2007. Internalization and dephosphorylation of connexin 43 in hypertrophied right ventricles of rats with pulmonary hypertension. *Circ J* **71**:382–389.
30. Shackley BS, Nguyen TP, Shivkumar K, Finn PJ, Fishbein MC. 2011. Idiopathic massive myocardial calcification: a case report and review of the literature. *Cardiovasc Pathol* **20**:e79–e83.
31. Swirski FK, Nahrendorf M, Etzrodt M, Wildgruber M, Cortez-Retamozo V, Panizzi P, Figueiredo JL, Kohler RH, Chudnovskiy A, Waterman P, Aikawa E, Mempel TR, Libby P, Weissleder R, Pittet MJ. 2009. Identification of splenic reservoir monocytes and their deployment to inflammatory sites. *Science* **325**: 612–616.
32. Zhao Y, Urganus AL, Spevak L, Shrestha S, Doty SB, Boskey AL, Pachman LM. 2009. Characterization of dystrophic calcification induced in mice by cardiotoxin. *Calcif Tissue Int* **85**: 267–275.